## Title

Stromal fibroblasts from perimenopausal endometrium exhibit a different transcriptome than those from the premenopausal endometrium



## Journal

Biology of Reproduction, 97(3)

## ISSN

0006-3363

## Authors

Erikson, David W
Barragan, Fatima
Piltonen, Terhi T
et al.

## Publication Date

2017-09-01

## DOI

10.1093/biolre/iox092

Peer reviewed

*Biology of Reproduction*, 2017, 97(3), 387–399
doi:10.1093/biolre/iox092
Research Article
Advance Access Publication Date: 19 August 2017

OXFORD

Research Article

# Stromal fibroblasts from perimenopausal endometrium exhibit a different transcriptome than those from the premenopausal endometrium†

**David W. Erikson[1], Fatima Barragan[1], Terhi T. Piltonen[1,2], Joseph C. Chen[1], Shaina Balayan[1], Juan C. Irwin[1] and Linda C. Giudice[1,*]**

[1]Department of Obstetrics, Gynecology, and Reproductive Sciences, University of California, San Francisco, San Francisco, California, USA and [2]Department of Obstetrics and Gynecology and Medical Research Center, Oulu University Hospital, University of Oulu, Oulu, Finland

*__Correspondence:__ Department of Obstetrics, Gynecology, and Reproductive Sciences, University of California, San Francisco, 505 Parnassus Ave, M1496, Box 0312, San Francisco, California 94143-0132, USA. E-mail: linda.giudice@ucsf.edu

†__Grant Support:__ This work was supported by the University of California, San Francisco Resource Allocation Program, the National Institutes of Health Eunice Kennedy Shriver National Institute of Child Health and Human Development Grant U54HD055764-06 Specialized Cooperative Centers Program in Reproduction and Infertility Research, the UCSF Research Allocation Program, the Ruth L. Kirchstein National Research Service Award 1F32HD074423-01, and the Sigrid Juselius Foundation, Academy of Finland, Finnish Medical Foundation, the Orion-Farmos Research Foundation, and the Maud Kuistila Foundation. The University of Virginia Center for Research in Reproduction Ligand Assay and Analysis Core is supported by the Eunice Kennedy Shriver NICHD/NIH (SCCPIR) Grant U54-HD28934.
__Conference Presentation:__ Presented in part at the 46th Annual Meeting of the Society for the Study of Reproduction, 22–26 July 2013, Montreal, Quebec.

Received 4 April 2017; Revised 24 July 2017; Accepted 17 August 2017

## Abstract

Human endometrium undergoes extensive regeneration on a cyclic basis in premenopausal women and likely occurs through the contribution of stem/progenitor cells. Menopause results in the permanent cessation of menstrual cycles and is preceded by perimenopause, a period of several years in which endocrine and biological changes occur and is a period of risk for endometrial proliferative disorders. The objectives of this study were to identify endometrial mesenchymal stem cells (eMSC) and endometrial stromal fibroblasts (eSF) in endometrium of perimenopausal women and perform expression profile analysis of perimenopausal eMSC and eSF to gain insight into the biology of stem/progenitor and lineage cell populations during the transition to menopause. Endometrial tissue was collected from perimenopausal and premenopausal women (n = 9 each). Microarray analysis was performed on fluorescence-activated cell sorting-isolated eSF and eMSC, and data were validated by quantitative real-time PCR. Principal component analysis showed that cells clustered into three distinct groups in 3-dimensional space: perimenopausal eMSC and premenopausal eMSC clustered together, while perimenopausal eSF and premenopausal eSF formed two discrete clusters separate from eMSC. Hierarchical clustering revealed a branching pattern consistent with principle clustering analysis results, indicating that eMSC from premenopausal and perimenopausal women exhibit similar transcriptomic signatures. Pathway analysis revealed dysregulation of cytoskeleton, proliferation, and survival pathways in perimenopausal vs.

premenopausal eSF. These data demonstrate that cell populations have altered gene expression in perimenopausal vs. premenopausal endometrium, and that perimenopausal eSF had altered pathway activation when compared to premenopausal eSF. This study provides insight into aging endometrium with relevance to function in reproductively older women.

## Summary Sentence

The hormonal milieu during the transition to menopause has an effect on endometrial stromal fibroblast gene expression and a minimal effect on the endometrial mesenchymal stem cell population, offering insight into the mechanisms by which the endometrium remains functional after menopause.

**Key words:** menopause, small nucleolar RNA, microarray, endometrial mesenchymal stem cell, fibroblast, endometrium.

## Introduction

Human endometrium undergoes extensive regeneration on a cyclic basis in response to estradiol (E2) and progesterone (P4) in premenopausal (PreM) women. This regeneration is likely to occur through the contribution of stem/progenitor cells of epithelial, mesenchymal, and endothelial lineages that aid in the regeneration of endometrium with each successive menstrual cycle [1–3]. Recently, a population of clonogenic, self-renewing, multipotent mesenchymal stem cells (MSC) co-expressing the markers cluster of differentiation 146 (CD146; melanoma cell adhesion molecule [MCAM]) and beta-type platelet-derived growth factor receptor (PDGFRB) was localized in the endometrium of PreM women [4–6]. Differential gene expression analysis of these endometrial mesenchymal stem cells (eMSC) revealed a clonogenic, multipotent cell that displayed both self-renewal pathways and the potential to differentiate into its lineage cell, the endometrial stromal fibroblast (eSF) [4]. Our group has subsequently demonstrated that eMSC are the parent cell of eSF and differentiate down the mesenchyme/fibroblast lineage in vitro [7].

Menopause, with depletion of ovarian follicular reserve, results in the permanent cessation of menstrual cycles [8]. This is preceded by a period of up to several years in which endocrine and biological changes occur. This period is often referred to as perimenopause, and lasts from the initiation of menstrual irregularities through 1 year after the cessation of menses [9]. During this time, ovulatory cycles are common, and the endometrium becomes stimulated by excessive E2 without opposing P4 production, leading to longer menstrual cycles [10–12]. For this reason, perimenopausal (PeriM) women are said to be in a "window of risk" for endometrial proliferative disorders such as endometrial polyps, hyperplasia, and epithelial and stromal cancer due to being exposed to prolonged unopposed estrogen in a tissue that has undergone up to 350 previous proliferative cycles [13].

With reproductive aging, postmenopausal endometrium is dormant but remains responsive to ovarian steroids, as evidenced by women undergoing hormone replacement therapy. Studies have demonstrated that reproductive aging is due to a decline in oocyte quantity as well as quality and not due to a diminished capacity of the endometrium to undergo embryo implantation [14,15]. Recently, eMSC were found to reside in postmenopausal endometrium and did not differ significantly from eMSC isolated from PreM women [16]. However, given that the endometrium does not experience a decreased functional capacity in the proper hormonal environment, it is of interest to determine if eSF from women undergoing the transition to menopause maintain the same genotype as their PreM counterparts, if eMSC persist in a functional capacity in the endometrium during perimenopause, and whether eMSC and eSF undergo changes as a result of the changing PeriM endocrine milieu. The objectives of this study were to identify eMSC and eSF in endometrium of PeriM women and perform expression profile analysis of PeriM eMSC and eSF to gain insight into the biology of these endometrial stem/progenitor and lineage cell populations during the transition to menopause.

## Materials and methods

### Study subjects and tissues

Tissue samples were procured through the National Institutes of Health (NIH)/University of California, San Francisco (UCSF) Human Endometrial Tissue and DNA Bank (http://obgyn.ucsf.edu/crs/tissue_bank) in accordance with the guidelines of the Declaration of Helsinki. Written, informed consent was obtained from all participants in the UCSF Center for Reproductive Health, and the study was approved by the UCSF Committee on Human Research. The clinical summary of the study participants is shown in Table 1. PeriM subjects (n = 94 554 yrs) had measured serum levels of anti-Müllerian hormone (AMH; a predictor of ovarian reserve) at or below 0.42 ng/ml (Table 1) as measured by the University of Virginia NIH National Centers for Translation and Infertility Centers Ligand Core. One PeriM subject who did not consent to blood collection was experiencing irregular cycles while another reported regular menstrual cycles. Both were included in the study analysis based on age and inclusion verified by clustering of their respective samples by principal component analysis (PCA) and hierarchical clustering (HC) with samples from other PeriM subjects. PreM subjects (n = 9; age 24–41 yrs) reported regular menstrual cycles or featured hormonal profiles indicative of proliferative phase. All samples were obtained from women undergoing benign gynecological surgery. Neither PeriM nor PreM subjects were exposed to hormonal medications for at least 2 months prior to tissue sampling and were confirmed to be not pregnant.

### Tissue processing and fluorescence-activated cell sorting of endometrial stromal cell populations

Tissue biopsies were divided into separate fresh samples and processed separately for fluorescence-activated cell sorting (FACS) and histological examination in optimal cutting temperature (OCT) compound. Tissue processing for FACS analysis was performed as previously described [4,17]. Briefly, enzymatically dissociated endometrial cells were incubated in blocking buffer (phosphate-buffered saline [PBS] containing 40% human serum and 1% bovine serum albumin [BSA]) for 30 min on ice and then labeled with the following fluorochrome-conjugated antibodies (BD Biosciences)

**Table 1.** Clinical characteristics of study subjects. PE, proliferative endometrium; PeriM, perimenopause; PreM, premenopause; E2, estradiol; P4, progesterone; AMH, anti-Müllerian hormone; BMI, body mass index.

| Subject ID | Study ID | Age[a] | Diagnosis | Race | Regular cycles | Menstrual cycle phase | E2[b] (pg/ml) | P4[c] (ng/ml) | AMH[d] (ng/ml) | BMI[e] |
|---|---|---|---|---|---|---|---|---|---|---|
| 1953 | PeriM 1 | 45 | Follicular/paratubal cysts | White | No | PE | 186.9 | 0.46 | 0.42 | 22.9 |
| 1961 | PeriM 2 | 48 | Fibroids | Black | Yes | Weak PE | 69.4 | 2.91 | <0.16 | 35.0 |
| 1852 | PeriM 3 | 48 | Symptomatic leiomyomas, adenomyosis, paratubal cysts, menorrhagia, dysmenorrhea | Black | Yes | Weak PE | 27.9 | 0.53 | <0.16 | 24.8 |
| 1930 | PeriM 4 | 49 | Menorrhagia, chronic pain, endocervical polyp | White | No | PE | 79.9 | 2.7 | <0.16 | 25.6 |
| 1931 | PeriM 5 | 47 | Menorrhagia, fibroids, adenomyosis suspected | White | No | PE | 344.8 | 0.86 | 0.33 | 39.3 |
| 1982 | PeriM 6 | 47 | Fibroids, mediastinal mass | Black | No | PE | – | – | – | 55.6 |
| 2003 | PeriM 7 | 45 | Menorrhagia, endometrial polyps | White | No | PE | 21.6 | 0.4 | <0.17 | 24.1 |
| 1889 | PeriM 8 | 48 | Adenomyosis, fibroids, menorrhagia | Asian | Yes | PE w/stromal breakdown | – | – | – | 24.8 |
| 1997 | PeriM 9 | 54 | Menorrhagia, right ovarian simple cyst | White | No | inactive | 13.6 | 0.45 | <0.16 | 38.0 |
| 2020 | PreM 1 | 24 | Natural cycle biopsy (volunteer) | White Hispanic | N/A | PE | 1389.4 | 0.96 | 8.5 | 23.1 |
| 2021 | PreM 2 | 25 | Natural cycle biopsy (volunteer) | Asian | N/A | PE | 47.5 | 1.33 | 3.3 | 23.0 |
| 1912 | PreM 3 | 28 | Left ovarian cyst, mature teratoma, adnexal mass consistent with dermoid | Asian | Yes | PE | – | – | – | 21.5 |
| 2008 | PreM 4 | 39 | Undesired fertility | Asian | N/A | PE | 198.3 | 0.81 | – | 24.3 |
| 2594 | PreM 5 | – | – | | | PE | 106.6 | 0.72 | 4.6 | 18.5 |
| 1807 | PreM 6 | 29 | Natural cycle biopsy (volunteer) | White | Yes | PE | 43.3 | – | 6.7 | 27.9 |
| 1911 | PreM 7 | 37 | Undesired fertility | Asian | Yes | PE | 61.4 | 0.38 | 0.27 | 32.4 |
| 1947 | PreM 8 | 36 | Fibroids, menorrhagia, dysmenorrhea, anemia, adenomyosis | Pacific Islander | Yes | PE | – | – | – | 44.0 |
| 1948 | PreM 9 | 41 | Benign endometrial polyp, menorrhagia, adenomyosis | Pacific Islander | Yes | PE | 62.7 | 2.79 | 1.1 | 51.5 |

[a]Age (mean ± s.d.): PeriM (47.9 ± 2.7 yrs); PreM (32.4 ± 6.6 yrs) ($P < 0.001$).
[b]E2 (mean ± s.e.m.): PeriM (106.3 ± 45.6 pg/ml); PreM (272.7 ± 187.2 pg/ml) ($P > 0.05$).
[c]P4 (mean ± s.e.m.): PeriM (1.19 ± 0.42 ng/ml); PreM (1.17 ± 0.32 ng/ml) ($P > 0.05$).
[d]AMH (mean ± s.e.m.): PeriM (0.22 ± 0.05 ng/ml); PreM (4.08 ± 1.03 ng/ml) ($P > 0.01$).
[e]BMI (mean ± s.e.m.): PeriM (32.3 ± 3.6); PreM (29.6 ± 3.7) ($P > 0.05$).

in PBS containing 10% human serum and 1% BSA: CD146 (or MCAM, CD146, fluorescein isothiocyanate anti-MCAM, clone P1H12) at 1:5 dilution to label perivascular/endothelial cells; PDGFRB(phycoerythrin anti-PDGFRB, clone J25-602) at 1:5 dilution to label eSF; cluster of differentiation 45 (CD45, phycoerythrin-Cy-7 anti-CD45, clone HI30) at 1:20 dilution to label leukocytes for removal; and epithelial cell (EC) adhesion molecule (EPCAM, allophycocyanin anti-EPCAM, clone EBA-1) at 1:20 dilution to label ECs for removal. The digested cell suspension was analyzed on a FACS Aria II with FACS Diva software (BD Biosciences). FACS-sorted cell pellets were stored at –80°C until used for RNA extraction. Tissue samples used for histological analysis were embedded in OCT, snap frozen in liquid nitrogen, and stored at –80°C until use for immunofluorescence analysis.

## RNA and cDNA preparation for microarray analysis and quantitative real-time PCR

Total RNA was isolated from FACS-sorted cell populations (eSF and eMSC) using the Arcturus PicoPure RNA isolation kit (Applied Biosystems, Life Technologies Corporation) following the manufacturer's instructions. An additional deoxyribonuclease treatment was performed using the ribonuclease-free deoxyribonuclease set (Qiagen). Reverse transcription and amplification of purified RNA into cDNA was performed using NuGEN WT-Ovation Exon FFPE System V2 (NuGEN). The integrity of resultant cDNA was assessed using an Agilent 2100 Bioanalyzer (Agilent Technologies), and individual samples meeting yield requirements and quality standards were further processed and hybridized to Affymetrix Human Gene 1.0 ST arrays (Affymetrix), probing 21 014 genes. Arrays were scanned according to the protocol described in the wild-type sense target labeling assay manual from Affymetrix (Version 4, FS450_0007).

## Biological functions and canonical pathway analysis

"Transcript cluster ID" and fold change data from up- and down-regulated genes in each comparison were imported into Ingenuity Pathway Analysis (IPA; Ingenuity Systems). Detailed pathway analysis was performed using the core analysis function in IPA to interpret data in the context of biological function, pathways, and networks. Biological functions are composed of molecular and cellular functions, and canonical pathways include signaling and metabolic pathways. Significance of biological functions and canonical pathways were tested by the Fisher exact test *P*-value [4].

### Validation of microarray analysis by microfluidic quantitative real-time PCR

Forty-three genes were chosen from the generated differential expression gene lists were chosen for validation based on their involvement in significant activation or suppression of select biological functions revealed in IPA analysis. A total of 33 cDNA samples from the FACS-sorted endometrial cell populations were analyzed in duplicate by quantitative real-time polymerase chain reaction (Q-RT-PCR) using the Fluidigm 48.48 dynamic array with integrated fluidic circuits and the BioMark HD system (Fluidigm, City, State) as previously described [4,17]. All procedures used the updated Fluidigm protocol 37, which included modifications to volume/concentration of reagents and timing of reactions for preamplification and BioMark quantitative PCR. Briefly, 200 ng cDNA was preamplified to generate a pool of target genes in 5 $\mu$l reactions using Taq-Man Pre-Amp master mix (Applied Biosystems) and 500 nM of each primer pair. Samples were then treated with exonuclease I (New England BioLabs), and samples were diluted 1:5 in Tris-ethylenediaminetetraacetic acid (Tris-EDTA) (TEKnova, Hollister, CA). Q-RT-PCR was performed using SsoFast Evagreen Supermix with low ROX binding dye (Biotium Inc) and a final primer concentration of 5 $\mu$M. Data were processed by user-detected threshold settings with linear baseline correction using BioMark real-time PCR analysis software (version 3.0.4). Melt curves were assessed using the melting temperature threshold.

Relative expression for each comparison was obtained using the comparative cycle threshold (Ct) method, in which the amount of target gene was normalized to beta-actin (ACTB) represented by $\Delta$Ct [4]. Expression was normalized to an internal calibrator for sorted cells ($\Delta\Delta$Ct) and relative expression calculated by $2^{-\Delta\Delta Ct}$ (ABI, http://hcgs.unh.edu/protocol/realtime/userbulletin2.pdf). Fold changes were calculated by comparing relative expression values using the same comparisons as in the differential gene expression analysis.

### Immunofluorescence

Immunofluorescence staining of frozen endometrial biopsy sections obtained from PeriM women to identify eMSC was performed as previously described [4]. Briefly, frozen sections (8 $\mu$M) were mounted on Superfrost/Plus slides (Fisher Scientific) and fixed in –20°C methanol for 10 min, and blocked in antibody dilution buffer (two parts PBS with 1% BSA, 0.3% Tween 20 [pH 8.0], and one part glycerol) containing 10% goat serum for 2 h at room temperature. Sections were washed and incubated overnight at 4°C with 5 $\mu$g/ml mouse anti-MCAM (CD146) IgG. Following three washes, sections were incubated with 8 $\mu$g/ml anti-mouse IgG Alexa 488 for 4 h at room temperature, and washed. Sections were then incubated overnight at 4°C with 5 $\mu$g/ml rabbit anti-PDGFRB IgG, washed and incubated with 8 $\mu$g/ml anti-rabbit IgG Alexa 594 for 4 h at 4°C. After additional washes, slides were dipped in distilled-deionized $H_2O$, overlaid with antifade mounting reagent containing DAPI (Invitrogen), and mounted with coverslips. Images at 200× magnification were captured on a Zeiss microscope fitted with a high-resolution Zeiss digital camera with Zeiss software (Zeiss). Figures were assembled using Adobe Photoshop Version 6.0 (Adobe Systems, San Jose, CA).

### Statistics

Microarray data analysis was performed using GeneSpring as previously described [4,17]. The intensity values of probe sets in the GeneChip operating software (Affymetrix) were imported into GeneSpring version 11.02 software (Agilent Technologies), normalized and subjected to $\log^2$ transformation using the robust multi-array analysis as the background correction algorithm for ST array technology. Pairwise comparisons of differentially expressed genes ($P < 0.05$, $\geq$1.5 FC) between different cell types or individual cell types between different age groups were performed using ANOVA with Tukey post hoc analysis and Benjamini–Hochberg multiple-testing correction for false discovery rate. An unbiased PCA algorithm was applied to all samples, using all 21 014 genes on the chip to identify similar expression patterns and visualize underlying cluster structures in 3-dimensional space. HC analysis was performed using differentially expressed genes with 2.0-fold or greater change difference from all samples and among all experimental conditions. The clustering algorithm used the Euclidean distance measure with the centroid linkage rule to identify samples with similar patterns of gene expression. For post array quantitative PCR analysis, data were analyzed by analysis of variance (ANOVA) utilizing Tukey post-hoc analysis with R commander (http://socserv.mcmaster.ca/jfox/Misc/Rcmdr). For pathway analysis of biological functions, IPA was used to identify pathways that were affected by differentially expressed genes in each treatment group with a >2.0-fold change. Identified pathways were analyzed for Z-scores to assess the activation (>2.0) or inhibition (<2.0) of respective pathways [18].

## Results

### Transcriptome analysis of endometrial mesenchymal stem cells and endometrial stromal fibroblast from perimenopausal and premenopausal women

The .cel files obtained from the microarray studies showing differential gene expression by age (PeriM versus PreM) and cell type (eMSC versus eSF) were uploaded to the Gene Expression Omnibus (GEO at the National Center for Biotechnology Information, http://www.ncbi.nlm.nih.gov/geo/; accession number GSE97163).

### Principal component analysis and hierarchical clustering of fluorescence-activated cell sorting-isolated endometrial cell populations

Five different cell populations from each sample were identified by FACS according to the fluorochrome-conjugated antibody labeling: CD45+ leukocytes, EPCAM+ ECs, CD146+/PDGFRB– endothelial cells, CD146–/PDGFRB+ eSF, and CD146+/PDGFRB+ eMSC. CD45+ and EPCAM+ cells were sorted out and not collected for the present study; only eSF and eMSC populations were analyzed herein. Analysis of microarray data from the two isolated cell types showed that they clustered into three distinct groups in 3-dimensional space by PCA (Figure 1A): PeriM eMSC and PreM eMSC clustered together, while PeriM eSF and PreM eSF formed discrete clusters separate from eMSC.

HC revealed an initial three-way branching separating PreM eSF from eMSC and PeriM eSF. A second branching separated eMSC from PeriM eSF. Within the eMSC sub-branch, the samples did not cluster distinctly by age group (PeriM or PreM), showing no clear segregation between the eMSC populations (Figure 1B), consistent with the unbiased PCA results (Figure 1A).

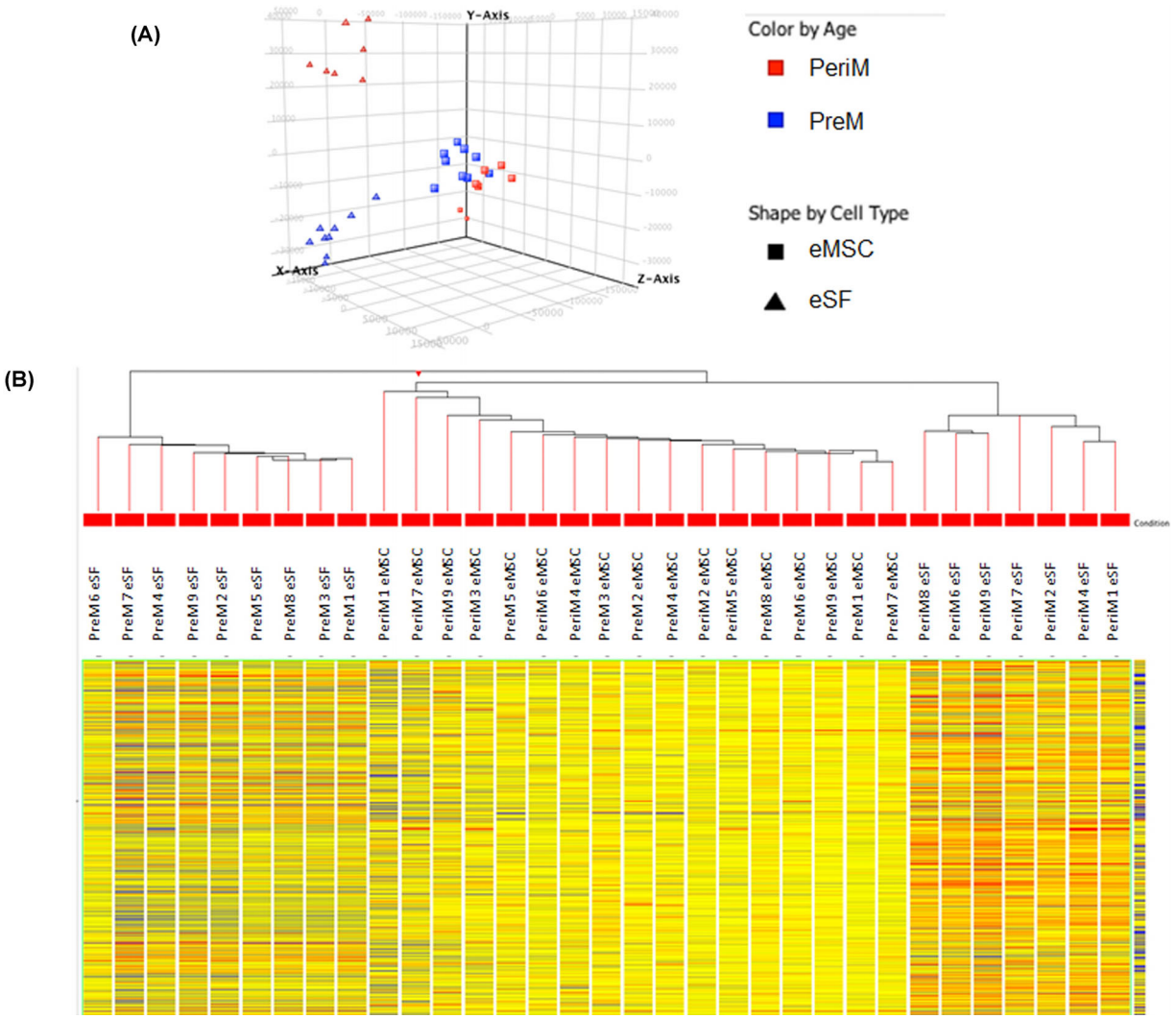


**Figure 1.** PCA and HC. (A) Endometrial cell populations from perimenopausal (PeriM) and premenopausal (PreM) women clustered in PCA by cell type, with endometrial mesenchymal stem cells (eMSC) from PeriM and PreM women clustering together, and endometrial stromal fibroblasts (eSF) forming two discrete clusters separate from eMSC. (B) HC analysis of the differentially expressed genes (≥2.0-fold change, $P < 0.05$) between eMSC and eSF in PeriM and PreM women.

## Differential expression and pathway analyses of fluorescence-activated cell sorting-isolated endometrial cell populations

The transcriptomes of isolated cell types were analyzed in the following gene expression comparisons: (1) PeriM eMSC vs. PreM eMSC; (2) PeriM eSF vs. PeriM eMSC; (3) PeriM eSF vs. PreM eSF ; and (4) PreM eMSC vs. PreM eSF (Supplemental Tables S1–S4). Selected genes appear in Table 2. Transcript cluster IDs from genes in the resultant lists were submitted for IPA analysis. The complete list of regulated biological pathways appears in Supplemental Tables S5–S8. From this list, pathways noted to be regulated between specific comparisons (Table 3) were used to select genes for Q-RT-PCR validation (Table 4).

## Differentially expressed genes

Resultant gene lists were generated using a 1.5-fold change threshold from the pairwise comparisons of differentially expressed genes [19–23]. There were 1066 differentially expressed genes in the PeriM eSF vs. PreM eSF comparison (704 up-regulated and 362 down-regulated), 145 differentially expressed genes in the PeriM eMSC vs. PreM eMSC comparison (17 up-regulated, 128 down-regulated), 645 differentially expressed genes in the PeriM eSF vs. PeriM eMSC comparison (575 up-regulated, 70 down-regulated), and 656 differentially expressed genes in the PreM eSF vs. PreM eMSC comparison (297 up-regulated, 359 down-regulated). The relationship between differentially expressed genes and comparisons can be seen in Figure 2. These data demonstrate, like the PCA and HC analyses, that the PeriM and PreM eMSC have more genes in common than PeriM eSF and PreM eSF. In addition, the number of differentially expressed genes between eSF and eMSC comparison are similar, regardless of age group (645 PeriM, 656 PreM).

## Ingenuity pathway analysis

IPA was based on two metrics, activation Z-score and *P*-value (Supplemental Tables S5–S8). Pathway analysis using transcript cluster IDs from the resultant gene lists revealed a number of regulated

**Table 2.** Select up- and down-regulated genes in eMSC and eSF from PeriM and PreM women.

| PeriM eSF vs. PeriM eMSC | | PeriM eMSC vs. PreM eMSC | | PeriM eSF vs. PreM eSF | | PreM eSF vs. PreM eMSC | |
|---|---|---|---|---|---|---|---|
| Gene symbol | FC | Gene symbol | FC | Gene symbol | FC | Gene symbol | FC |
| *ASAM* | 8.1 | *SNORD113-3* | 2.7 | *VTRNA1-3* | 12.2 | *PLA2G7\|TDRD6* | 18.5 |
| *SNORA28* | 7.0 | *SNORD116-1* | 2.6 | *RPPH1* | 12.0 | *PAGE4* | 6.9 |
| *VTRNA1-3* | 6.7 | *SNORA42* | 2.5 | *BGN* | 9.0 | *SLC27A6* | 6.9 |
| *SNORA48* | 6.6 | *SNORD116-4\|SNRPN* | 2.4 | *SNORA48* | 8.4 | *ROBO2* | 6.4 |
| *FBLN5* | 5.5 | *RPPH1* | 2.3 | *HIST1H1E* | 8.4 | *SNORD114-2* | 5.7 |
| *MMP2* | 5.2 | *DSERG1* | 2.1 | *SNORA28* | 6.7 | *LRRTM4* | 5.4 |
| *TGM2* | 4.7 | *SNORD114-2* | 2.0 | *MMP14* | 5.8 | *PAPPA\|PAPPAS* | 4.7 |
| *MMP14* | 4.6 | *SNORD114-26* | 1.7 | *FOS* | 5.2 | *FGF9* | 4.4 |
| *HOXA11* | 4.2 | *PAPPA\|PAPPAS* | 1.6 | *MIF\|SLC2A11* | 4.8 | *SNORD113-3* | 4.3 |
| *LCP1* | 4.0 | *ITGA5* | 1.5 | *ITGA5* | 4.5 | *SNORD114-26* | 2.7 |
| *SNORD34\|RPL13A* | 3.7 | *MMP2* | –1.5 | *SERPING1* | 4.3 | *FBLN5* | 2.1 |
| *SNORA5A* | 3.2 | *FBLN5* | –1.8 | *SNORA5A* | 4.0 | *LCP1* | 1.8 |
| *FOS* | 3.2 | *TUBB* | –1.8 | *MIR27B\|C9orf3* | 4.0 | *SNORD68\|RPL13* | 1.8 |
| *PTGDS* | 3.1 | *LCP1* | –1.8 | *FLNA* | 3.9 | *SNORD116-4\|SNRPN* | 1.7 |
| *EGFR* | 3.0 | *FBLN1* | –1.9 | *TGM2* | 3.9 | *SNORD116-1* | 1.6 |
| *SNORD68\|RPL13* | 2.8 | *HTR1F* | –2.6 | *SNORD34\|RPL13A* | 3.5 | *SNORD73A* | 1.5 |
| *FBLN1* | 2.5 | *HIST1H2AE* | –2.6 | *MMP2* | 3.3 | *MAPK3* | –1.5 |
| *SERPING1* | 2.5 | *JOSD1* | –2.7 | *TUBB* | 3.3 | *BMP1* | –1.5 |
| *ITGA5* | 2.4 | *THBS4* | –3.2 | *GRN* | 3.3 | *ELOVL1* | –1.5 |
| *MIF\|SLC2A11* | 2.4 | *ELOVL2* | –3.9 | *MAPK3* | 3.1 | *MMP14* | –1.6 |
| *GRN* | 2.2 | | | *CST3* | 3.0 | *ILK* | –1.6 |
| *SNORA70\|RPL10* | 2.2 | | | *ELOVL1* | 3.0 | *GRN* | –1.6 |
| *VTRNA1-2* | 2.2 | | | *CTSA* | 2.9 | *CTSA* | –1.6 |
| *TIMP2* | 2.0 | | | *RHOC* | 2.7 | *MIF\|SLC2A11* | –2.3 |
| *TUBB* | 2.0 | | | *HOXA11* | 2.6 | *NOTCH1* | –2.4 |
| *SNORD35A\|RPL13A* | 2.0 | | | *A2M* | 2.5 | *FLNA* | –2.7 |
| *MAPK3* | 2.0 | | | *ILK* | 2.3 | *CCND1* | –2.8 |
| *FLNA* | 1.9 | | | *TGFB1* | 2.3 | *TUBB* | –2.9 |
| *RHOC* | 1.8 | | | *TIMP2* | 2.3 | *NOTCH3* | –2.9 |
| *PAPPA\|PAPPAS* | 1.7 | | | *SNORD35A\|RPL13A* | 2.3 | *HEYL* | –5.1 |
| *CTSA* | 1.7 | | | *BMP1* | 2.3 | *SLIT2* | –6.8 |
| *BMP1* | 1.6 | | | *SNORA70\|RPL10* | 2.2 | *A2M* | –8.4 |
| *ILK* | 1.6 | | | *CCND1* | 2.0 | *ACTA2* | –8.6 |
| *ARID1B* | 1.5 | | | *NOTCH1* | 2.0 | *ELOVL2* | –9.7 |
| *SNORD42A* | –1.8 | | | *EGFR* | 1.7 | *HTR1F* | –10.6 |
| *SNORD47\|GAS5* | –1.9 | | | *HEYL* | 1.6 | *LPL* | –10.7 |
| *NOTCH3* | –2.0 | | | *FBLN5* | 1.5 | *BGN* | –12.1 |
| *BCL2* | –2.3 | | | *SNORD114-26* | –1.7 | | |
| *SNORD73A* | –2.5 | | | *BCL2* | –1.8 | | |
| *A2M* | –2.6 | | | *SNORD116-4\|SNRPN* | –2.2 | | |
| *HEYL* | –2.6 | | | *SNORD116-1* | –2.2 | | |
| *SNORA42* | –2.7 | | | *SNORD47\|GAS5* | –2.3 | | |
| *ELOVL2* | –2.9 | | | *SNORD42A* | –2.4 | | |
| *SNORD116-4\|SNRPN* | –3.1 | | | *SNORD114-2* | –2.6 | | |
| *SNORD116-1* | –3.6 | | | *CDH10* | –3.3 | | |
| *PTP4A3* | –3.7 | | | *SNORD73A* | –3.9 | | |
| *LPL* | –3.7 | | | *MAGT1* | –4.5 | | |
| *UACA* | –3.8 | | | *CETN3* | –4.5 | | |
| *HTR1F* | –4.5 | | | *NME7* | –4.6 | | |
| | | | | *UBLCP1* | –5.0 | | |
| | | | | *PLA2G7\|TDRD6* | –5.3 | | |

biological pathways. Significant activation of a pathway was predicted with an activation Z-score > 2.0; significant suppression of a pathway was predicted with an activation Z-score <-2.0 [19]. There were 52 regulated pathways in the PeriM eSF vs. PreM eSF comparison; 46 regulated pathways in the PreM eSF vs. PreM eMSC comparison; and 75 regulated pathways in the PeriM eSF vs. PeriM eMSC comparison. There were no regulated biological pathways in the PeriM eMSC vs. PreM eMSC comparison, which is not surprising given the relatively small number of differentially regulated genes between these two groups and highlighting the similarity in gene expression of these two groups revealed by PCA and HC. A subset of regulated pathways that appeared within several comparisons was generated and is shown in Table 3. These include organization of cytoskeleton, fibrogenesis, formation of filaments, metabolism of protein, cell spreading, formation of actin stress fibers, migration of fibroblast cell lines, cell transformation, proliferation of fibroblasts, formation of cytoskeleton, and organismal death.

**Table 3.** Select predicted activated (z-score ≥ 2.0) and predicted suppressed (z-score ≤ –2.0) pathways from IPA based on differentially expressed gene lists.

| Functions Annotation | PeriM eSF vs. PreM eSF | PeriM eSF vs PeriM eMSC | PreM eSF vs PreM eMSC | Validated Molecules |
|---|---|---|---|---|
| Organization of cytoskeleton | 3.18 (107) | 2.58 (65) | –2.04 (83) | *A2M, FGF9, FLNA, FOS, GRN, ILK, MAPK3, NOTCH1, RHOC, TGFB1, TUBB* |
| Fibrogenesis | 3.68 (45) | – | –2.76 (31) | *A2M, EGFR, MIF, MMP2, PTGDS, RHOC, SERPING1, TGFB1, TUBB* |
| Formation of filaments | 3.88 (44) | – | –2.97 (30) | *A2M, EGFR, MIF, MMP2, RHOC, SERPING1, TGFB1, TUBB* |
| Metabolism of protein | 2.30 (89) | – | – | *BCL2, BMP1, CCND1, CST3, EGFR, FLNA, FOS, MAPK3, MMP14, MMP2, NOTCH1, TGFB1, TGM2, TIMP2* |
| Cell spreading | 3.72 (32) | 2.20 (23) | – | *A2M, EGFR, FLNA, ILK, ITGA5, MAPK3, MMP14, TGFB1* |
| Formation of actin stress fibers | 3.69 (27) | – | –2.91 (17) | *EGFR, MIF, MMP2, RHOC, TGFB1* |
| Migration of fibroblast cell lines | 3.18 (15) | 2.88 (12) | – | *EGFR, ITGA5, MMP14, PTGDS, TGM2* |
| Cell transformation | 2.58 (49) | 2.55 (34) | – | *BCL2, CCND1, EGFR, FOS, HEYL, ILK, MIF, MMP2, NOTCH1, TGFB1* |
| Proliferation of fibroblasts | 2.70 (42) | 2.45 (24) | –2.26 (32) | *CCND1, EGFR, FOS, GRN, ILK, ITGA5, MAPK3, MIF, MMP14, MMP2, TGFB1* |
| Formation of cytoskeleton | 3.81 (42) | 2.78 (25) | – | *EGFR, FLNA, MIF, MMP2, PTGDS, RHOC, TGFB1, TUBB* |
| Organismal death | –7.82 (207) | –7.76 (136) | – | *BCL2, BGN, BMP1, CTSA, EGFR, FGF9, FLNA, FOS, GRN, HEYL, HOXA11, ILK, ITGA5, MAPK3, MIF, MMP14, MMP2, SERPING1, TGM2, TIMP2* |

### Validation of select genes by quantitative real-time PCR

Using a microfluidic approach to quantitative PCR allowed us to analyze 43 genes across 33 cell isolates simultaneously. The results for validation of select genes are shown in Table 4. Genes were chosen for validation based on their involvement in selected significantly regulated biological pathways.

A finding of note is the differential expression of a number of small nucleolar RNA C/D box (SNORD) and small nucleolar RNA H/ACA box (SNORA) genes across several different comparisons in the study (Table 5). These include among the most highly upregulated genes in PeriM eMSC vs. PreM eMSC (*SNORD113-3*, *116-1*, *114-2*, *114-26*, and *SNORA42*), PeriM eSF vs. PeriM eMSC (*SNORA28*, *48*). We also investigated estrogen receptor alpha (*ESR1*), estrogen receptor beta (*ESR2*), and progesterone receptor (*PGR*) by Q-RT-PCR to gain insight into the potential for ovarian hormonal regulation of eSF and eMSC. *PGR* was up-regulated in all eSF vs. eMSC comparisons, and up-regulated in all PeriM vs. PreM comparisons. *ESR1* was down-regulated in all PeriM vs. PreM comparisons, but up-regulated in eSF vs. eMSC comparisons. *ESR2* showed a more complex regulation, with highest up-regulation in PeriM eSF vs. PreM eSF and greatest downregulation in PreM eSF vs. PreM eMSC. CD146, the marker used to select between eMSC and eSF, was not differentially expressed in the array analysis, most likely due to variability in expression by eMSC collected from different subjects. Analysis with Q-RT-PCR, however, revealed an 18.6-fold down-regulation in PeriM eSF vs. PeriM eMSC and a 3106.5-fold down-regulation in PreM eSF vs. PreM eMSC as anticipated. Of note is the up-regulation of CD146 in PeriM eSF vs. PreM eSF (893.2-fold), supporting the PCA and HC data demonstrating that PeriM eSF cluster more closely to the eMSC populations than PreM eSF.

### Localization of endometrial mesenchymal stem cells in perimenopausal endometrium

We previously demonstrated the localization of eMSC in the perivascular region around small blood vessels in PreM endometrium [4]. In the present study, FACS analysis revealed a population of endometrial cells that co-express CD146 and PDGFRB in PeriM endometrial tissue digests. Sections of PeriM endometrial biopsies embedded in OCT were analyzed for the presence of CD146 and PDGFRB by indirect immunofluorescence. CD146 localized to perivascular and endothelial cells in the endometrium (Figure 3), while PDGFRB localized to both endometrial stromal cells and perivascular cells (Figure 3). Neither CD146 nor PDGFRB were observed in endometrial glandular epithelium. CD146+/PDGFRB+ cells were identified in the perivascular region around small blood vessels in PeriM endometrium, confirming the presence of eMSC in PeriM endometrium. These results are similar to those previously found in PreM endometrium [4,6], where eMSC were also localized to the perivascular region in human endometrium.

We also evaluated the ratio of eMSC:eSF in PeriM endometrium and PreM endometrium to investigate the possibility of increased numbers of eMSC in PeriM endometrium. The ratio of eMSC:eSF in PeriM endometrium (0.033 ± 0.016) was not significantly different than that of PreM endometrium (0.024 ± 0.005) following analysis by FACS ($P > 0.05$) (data not shown).

## Discussion

### Endometrial mesenchymal stem cells and endometrial stromal fibroblast in peri and premenopausal women

This report provides the first differential gene expression analysis in endometrial cell populations from women undergoing the transition to menopause compared to PreM women. In addition, we have identified eMSC in PeriM women and have gained insight into the effect of the changing hormonal milieu in vivo on endometrial cells, namely eSF and eMSC, in these women. Interestingly, our results indicate that eMSCs from PreM and PeriM women exhibit a similar transcriptomic signature, while PeriM eSF exhibit pathway changes suggesting an aging cellular phenotype compared to PreM eSF.

### Peri and premenopausal endometrial mesenchymal stem cells

PCA revealed that the eMSC populations from PeriM and PreM women clustered together, and gene profiling analysis revealed

**Table 4.** Microfluidic Q-RT-PCR validation of differentially expressed genes between eMSC and eSF from PeriM and PreM women.

| | PeriM eSF vs. PreM eSF | | PeriM eMSC vs. PreM eMSC | | PeriM eSF vs.PeriM eMSC | | PreM eSF vs.PreM eMSC | |
|---|---|---|---|---|---|---|---|---|
| Gene | Microarray | Q-RT-PCR | Microarray | Q-RT-PCR | Microarray | Q-RT-PCR | Microarray | Q-RT-PCR |
| *A2M* | 2.5 | –1.1 | NC | 1.7 | –2.6 | –2.2 | –8.4 | –1.1 |
| *BCL2* | –1.8 | –4.6 | NC | 5.0 | –2.3 | –11.5 | NC | 2.0 |
| *BGN* | 9.0 | 9.4 | NC | 1.3 | NC | –1.9 | –12.1 | –13.7 |
| *BMP1* | 2.3 | 678.2 | NC | 6.3 | 1.6 | 3.9 | –1.5 | –28.1 |
| *CCND1* | 2.0 | 116.5 | NC | 1.5 | NC | 1.7 | –2.8 | –47.6 |
| *CD146* | NC | 893.2 | NC | 5.3 | NC | –18.6 | NC | –3106.5 |
| *CST3* | 3.0 | 116.5 | NC | 3.1 | NC | –1.0 | –2.2 | –257.4 |
| *CTSA* | 2.9 | 1.5 | NC | 1.3 | 1.7 | 2.8 | –1.6 | 2.4 |
| *EGFR* | 1.7 | 27.1 | NC | –1.4 | 3.0 | 8.7 | NC | –4.4 |
| *ESR1* | NC | –3.8 | NC | –1.4 | NC | 5.0 | NC | 13.4 |
| *ESR2* | NC | 14.7 | NC | –2.4 | NC | 1.0 | NC | –34.6 |
| *FGF9* | –3.3 | –1.0 | NC | 229.8 | NC | 2.1 | 4.4 | 513.6 |
| *FLNA* | 3.9 | 1502.7 | NC | 3.9 | 1.9 | –1.0 | –2.7 | –384.8 |
| *FOS* | 5.2 | 41.2 | NC | 1.9 | 3.2 | 2.1 | –1.8 | –10.4 |
| *GRN* | 3.3 | 26.4 | NC | 1.8 | 2.2 | 2.8 | –1.6 | –5.3 |
| *HEYL* | 1.6 | 78.0 | NC | 2.0 | –2.6 | –3.9 | –5.1 | –149.1 |
| *HOXA11* | 2.6 | 180.8 | NC | 16.7 | 4.2 | 3.8 | NC | –2.8 |
| *ILK* | 2.3 | 460.0 | NC | 12.0 | 1.6 | 2.1 | –1.6 | –18.3 |
| *ITGA5* | 4.5 | 25 816.5 | 1.5 | 21.1 | 2.4 | 5.4 | NC | –225.5 |
| *MAPK3* | 3.1 | –2.6 | NC | –1.2 | 2.0 | 1.2 | –1.5 | 2.4 |
| *MIF* | 4.8 | 63.4 | NC | 1.4 | 2.4 | 1.2 | –2.3 | –38.4 |
| *MMP14* | 5.8 | 108.2 | NC | 1.2 | 4.6 | 10.2 | –1.6 | –9.1 |
| *MMP2* | 3.3 | 10.2 | –1.5 | –1.1 | 5.2 | 16.2 | NC | 1.5 |
| *NOTCH1* | 2.0 | 25.2 | NC | –1.0 | NC | –1.1 | –2.4 | –27.6 |
| *PDGFRB* | NC | 42.4 | NC | –1.2 | NC | 1.1 | NC | –48.2 |
| *PGR* | NC | 17.2 | NC | 22.2 | NC | 10.0 | NC | 12.9 |
| *PTGDS* | 2.4 | 4.8 | NC | 2.2 | 3.1 | 54.9 | NC | 25.4 |
| *RHOC* | 2.7 | 1143.6 | NC | 4.1 | 1.8 | 3.0 | –2.0 | –91.6 |
| *SERPING1* | 4.3 | 23.7 | NC | 3.7 | 2.5 | 2.2 | NC | –2.9 |
| *SNORA28* | 6.7 | 11 050.2 | NC | 28.2 | 7.0 | 8.7 | NC | –45.2 |
| *SNORA42* | NC | 50.2 | 2.5 | 2.4 | –2.7 | 8.3 | NC | –2.5 |
| *SNORA48* | 8.4 | 14.1 | NC | 11.2 | 6.6 | 2.6 | NC | 2.0 |
| *SNORD113-3* | NC | –4.7 | 2.7 | 9.7 | NC | 3.7 | 4.3 | 172.6 |
| *SNORD114-2* | –2.6 | 1.1 | 2.0 | 49.6 | NC | 3.4 | 5.7 | 149.2 |
| *SNORD114-26* | –1.7 | –3.0 | 1.7 | 12.6 | NC | 1.9 | 2.7 | 73.5 |
| *SNORD116-1* | –2.2 | –19.1 | 2.6 | 83.1 | –3.6 | –4.2 | 1.6 | 374.8 |
| *SNORD116-4* | –2.2 | 542.8 | 2.4 | 60.9 | –3.1 | –2.0 | 1.7 | –17.4 |
| *SNORD34* | 3.5 | –1.9 | NC | –1.6 | NC | 5.1 | NC | 6.0 |
| *TGFB1* | 2.3 | 12.2 | NC | 3.2 | NC | –1.1 | –2.0 | –4.2 |
| *TGM2* | 3.9 | 65.7 | NC | 2.8 | 4.7 | 6.3 | NC | –3.7 |
| *TIMP2* | 2.3 | 141.4 | NC | 2.8 | 2.0 | 3.5 | NC | –14.8 |
| *TUBB* | 3.3 | 1.5 | –1.8 | –1.5 | 2.0 | 1.8 | –2.9 | –1.3 |
| *VTRNA1-3* | 12.2 | 344.7 | NC | 12.9 | 6.7 | 3.8 | NC | –6.9 |

that this comparison contained the fewest number of differentially expressed genes amongst those investigated in this study. Together, these data suggest that eMSC are not dramatically different from women in either age group studied herein, and that the changing hormonal environment in PeriM did not have an effect on eMSC gene expression when compared to PreM women.

A recent study demonstrated that eMSC collected from postmenopausal women demonstrated similar clonogenicity, multipotency, and surface molecule phenotype whether or not, the subjects were treated with E2 prior to collection [16]. In addition, eMSC from postmenopausal women in the same study demonstrated similar self-renewal and eMSC marker expression as PreM eMSC [16]. These data support our observation that eMSC from PeriM women contain a similar transcriptome to those found in PreM women.

### Peri and premenopausal endometrial stromal fibroblast

PCA revealed eSF from PeriM and PreM women clustered into two distinct and separate groups from the eMSC. When comparing PeriM eSF to PreM eSF in the gene profiling analysis, the largest number of differentially expressed genes resulted from this comparison. PeriM eSF also branched more closely to the eMSC groups in the HC analysis, suggesting the PeriM eSF were more similar in gene expression profile to the eMSC than PreM eSF. Genes previously shown to be more highly expressed in eMSC than eSF from PreM women, including members of the Notch (Notch

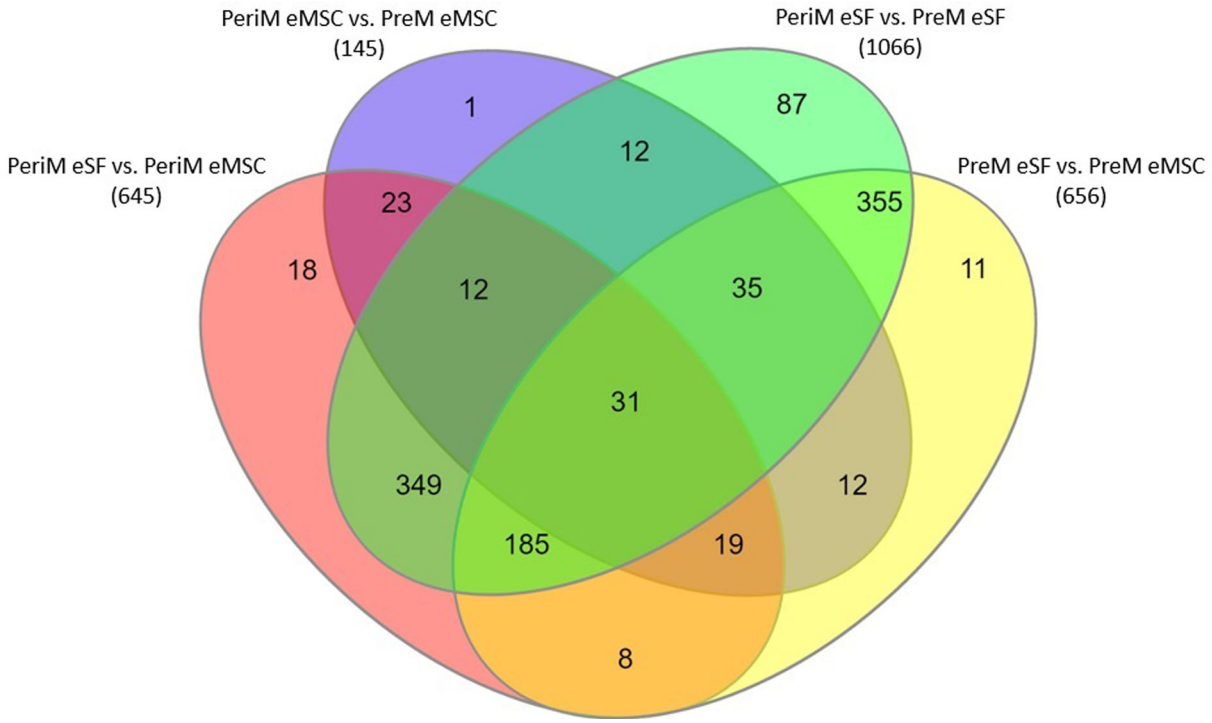


**Figure 2.** Differentially expressed genes from experimental groups. Venn diagram showing overlap of differentially expressed genes ($P < 0.05$, >1.5-fold change or <-1.5-fold change) between eSF and eMSC from PreM and PeriM women immediately after FACS isolation [38].

**Table 5.** Differential expression of small nucleolar RNA and vault RNA in eMSC and eSF from PeriM and PreM women.

| Gene | PeriM eSF vs. PreM eSF | PeriM eMSC vs. PreM eMSC | PeriM eSF vs. PeriM eMSC | PreM eSF vs. PreM eMSC |
|---|---|---|---|---|
| *SNORD34* | 3.5 | – | 3.7 | – |
| *SNORD35A* | 2.3 | – | 2.0 | – |
| *SNORD47* | –2.3 | – | –1.9 | – |
| *SNORD68* | – | – | 2.8 | 1.8 |
| *SNORD73A* | –3.9 | – | –2.5 | 1.5 |
| *SNORD113-3* | – | 2.7 | – | 4.3 |
| *SNORD114-2* | –2.6 | 2.0 | – | 5.7 |
| *SNORD114-26* | –1.7 | 1.7 | – | 2.7 |
| *SNORD116-1* | –2.2 | 2.6 | –3.6 | 1.6 |
| *SNORD116-4* | –2.2 | 2.4 | –3.1 | 1.7 |
| *SNORA5A* | 4.0 | – | 3.2 | – |
| *SNORA28* | 6.7 | – | 7.0 | – |
| *SNORA42* | – | 2.5 | –2.7 | – |
| *SNORA48* | 8.4 | – | 6.6 | – |
| *VTRNA1-3* | 12.2 | – | 6.7 | – |

SNORA, small nucleolar RNA H/ACA box; SNORD, small nucleolar RNA C/D box; VTRNA, vault RNA.

homolog 1 [*NOTCH1*], Hairy/enhancer-of-split related with YRPW motif-like protein [*HEYL*]) and transforming growth factor beta (transforming growth factor beta 1 [*TGFB1*] families [4] are more highly expressed in PeriM eSF than PreM eSF in the present study (Table 1). In addition, expression of CD146, the marker that differentiates eMSC from eSF in our FACS isolation protocol, shows an almost 900-fold increase in expression in PeriM eSF vs. PreM eSF by Q-RT-PCR (Table 3). This data suggest that the PeriM eSF exist in a less fully differentiated state more similar to eMSC than PreM eSF. Furthermore, this study identifies enhanced survival characteristics in the eSF from PeriM women, which may have important implications for endometrial pathologies in women later in life.

## Steroid hormone receptors

In the endometrium, eSF regulate EC proliferation and differentiation during development, and one of the eSF's main roles in adult endometrium is to regulate effects of E2 on EC [24], with eSF dysfunction potentially affecting epithelial function. While a previous study did not find any changes in hormone receptor expression in menopausal eMSC [16], and we did not find these changes by

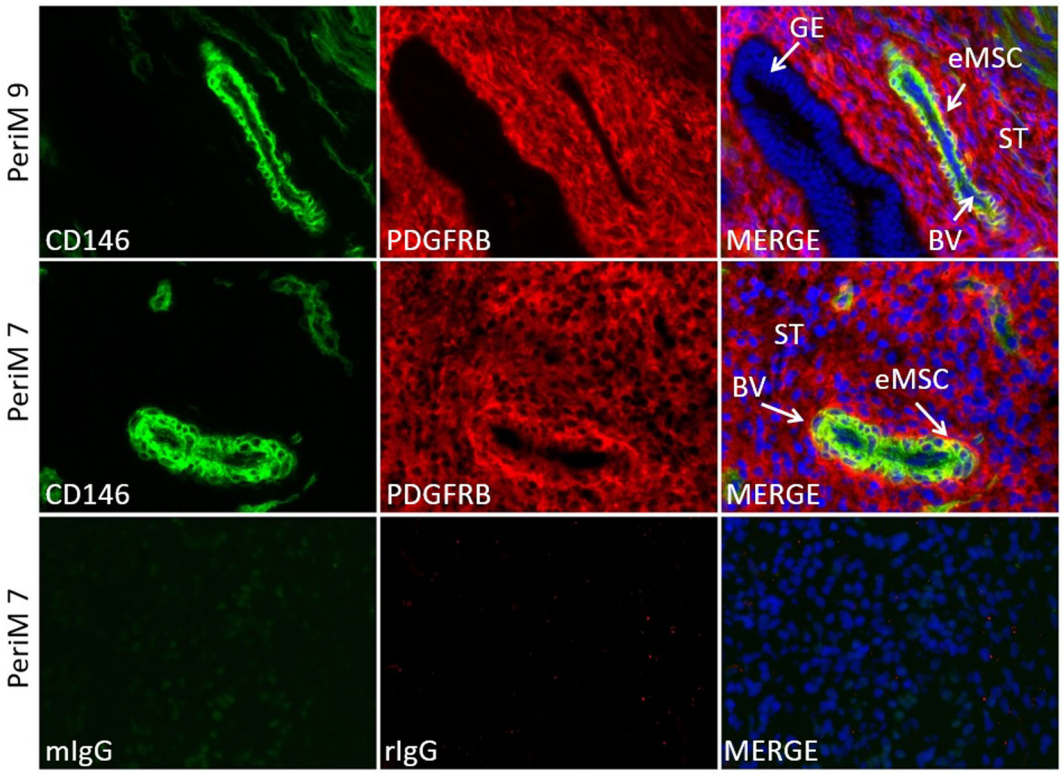


**Figure 3.** Localization of eMSC in PeriM endometrium by indirect immunofluorescence. Sections of endometrial biopsies from PeriM women were labeled for CD146 and PDGFRB. CD146 was localized to all perivascular cells, whereas PDGFRB showed a wider distribution on endometrial stromal cells as well as some perivascular cells. Staining for PDGFRB was absent in glandular epithelial cells. Colocalization of CD146 and PDGFRB (eMSC; arrow) was observed in a perivascular location. GE, glandular epithelium; BV, blood vessel; ST, stroma; eMSC, endometrial mesenchymal stem cell. Original magnification ×100.

microarray analysis, we did identify differences in *ESR1*, *ESR2*, and *PGR* expression by Q-RT-PCR. Progesterone receptor showed consistent patterns across comparisons, being more highly expressed in eSF than eMSC independent of age group (Table 3). However, the fold change was greatest in PeriM eMSC vs. PreM eMSC (22.2) and PeriM eSF vs. PreM eSF (17.2). This could be due to the effect of an inadequate opposition of E2 on the endometrium by P4, due to the lengthening and irregular menstrual cycles often seen during the transition to menopause [10–12], perhaps resulting in an E2-stimulated increase in *PGR* expression [25,26]. The differential expression of *ESR1* and *ESR2* revealed upregulation in eSF vs. eMSC (5.0 in PeriM; 13.4 in PreM), perhaps suggesting that fully mature eSF acquire the ability to respond to E2 during differentiation from the progenitor eMSC. Endometrial MSC (W5C5+ cells) isolated from postmenopausal endometrium did not express ER$\alpha$ and did not respond to systemic estrogen prior to sampling [16], suggesting that E2 may act on eMSC through surrounding niche cells [27]. Our data support these observations; while we did not investigate *ESR1* or *ESR2* expression on eMSC niche cells, we did see decreased gene expression of *ESR1* in PeriM vs. PreM in both eMSC (–1.4-fold change) and eSF (–3.8-fold change).

*ESR2*, on the other hand, is expressed in developing uterine tissues [28] and in vascular endothelium of adult endometrium [29]. To our knowledge, there has not been a previous report of *ESR2* expression in eMSC. In the current study, we found a significant increase in differential expression of *ESR2* in PeriM vs. PreM eSF (14.7). While we cannot deduce much about the expression levels or activity of this receptor based on these differential expression data, the observation is nonetheless intriguing. There is evidence that *ESR2* plays a role in some uterine diseases such as endometriosis [30] and leiomyoma [31] and may play a role in uterine elasticity in postmenopausal women [28].

The role of *ESR1* and *ESR2* in the PreM and PeriM endometrium with regard to eMSC and eSF function is, however, unclear and warrants further investigation. In sum, these data argue for PeriM eSF having characteristics of senescent cells that may affect the way eSF and eMSC respond to the changing hormonal environment in perimenopause.

## Pathway analyses

The similarity of PeriM eSF to eMSC is further indicated by pathways revealed by IPA, including predicted activation for formation of filaments, formation of cytoskeleton, organization of cytoskeleton, and formation of actin stress fibers. Recent work has demonstrated that MSC differentiation is highly dependent upon mechanical forces affecting the cell, and that in vitro regulation of these forces can affect changes upon the cytoskeleton to drive differentiation down osteogenic, chondrogenic, and adipogenic lineage pathways [32]. While these observations in and of themselves do not constitute evidence for an eMSC-like phenotype for the PeriM eSF, they do suggest that PeriM eSF have the potential to respond to mechanical forces similar to MSC, and may exist in a less-differentiated state in the PeriM endometrium. This may also explain, in part, why PeriM eSF exhibit an anti-apoptotic phenotype compared to PreM eSF.

Among our findings are regulated pathways and differentially expressed genes that are suggestive of a population of senescent cells or cells similar to senescent cells. Cellular senescence is the growth arrest that occurs in cells when they are exposed to oncogenic stress and is a mechanism to prevent the proliferation of potential cancer cells [33]. While the transcriptome of the PeriM eSF in the current study does not wholly represent that of a senescent cell population, the down-regulation of organismal death pathways (Table 2), increased matrix metalloproteinase (MMP) expression (Table 1), and increased EGFR expression (Table 1) are all common with senescent or aging cells [33]. These pathways also have overlap with age-related changes in tissues that make them more permissive to tumor growth [33].

### Small nucleolar RNAs

Gene profile analysis revealed a number of small nucleolar RNAs in the lists of differentially expressed genes by comparison (Table 4). The small nucleolar RNAs act as guide RNAs for chemical modification of ribosomal, transfer, and small nuclear RNAs and are found in two classes: H/ACA box (SNORA) associated with methylation and C/D box (SNORD) associated with pseudouridylation. They are emerging as important regulators of cellular function and disease development. Noncoding RNAs, including SNORAs/SNORDs have recently drawn interest for their roles in cellular carcinogenicity [34]. While the exact roles of the specific SNORAs/SNORDs identified in the current study remain largely undefined, a growing number of these molecules has been found to exhibit differential expression patterns in a number of cancers and demonstrate roles in cell transformation, tumorigenesis, and cellular metastasis [34]. In addition, SNORAs have been found to act in tumor suppression pathways, and may be capable of modifying the expression and function of p53, a tumor suppressor gene that is the most common target of genetic modification in cancer [34–36]. Of interest in our data, is the differential expression by comparison of the SNORA/SNORD molecules (Table 4) and the inverse fold changes found based on PreM or PeriM status. For example, *SNORD116-1* is decreased in PeriM eSF vs. PreM eSF (–2.2) and PeriM eSF vs. PeriM eMSC (–3.6), but increased in PeriM eMSC vs. PreM eMSC (2.6) and PreM eSF vs. PreM eMSC (1.7). While there is currently no report of noncoding RNAs acting to affect carcinogenic changes in PeriM or postmenopausal endometrium, it is possible that the differential expression of the SNORA/SNORD molecules is involved in altered regulation of RNA methylation and pseudouridylation in eSF and eMSC as the endometrium is transitioning to menopause. However, the significance behind these differential expressing patterns is unclear. A recent study on aging cartilage also identified a large number of differentially expressed SNORA molecules, but the authors were also unable to draw a conclusive link between the aging cells and differential expression of these molecules [37,38]. The observation of differential expression of SNORA molecules in the current study provides an interesting avenue of study of aging endometrial function, including pregnancy establishment, maintenance, placentation, and endometrial cancer.

### Role of uterine pathologies

The contribution of uterine pathologies to differences in gene expression between PeriM and PreM eSF is also worthy of discussion. Previous studies from our laboratory demonstrate gene expression differences in eMSC and eSF with the presence of pelvic inflammatory disease, namely polysystic ovary syndrome and endometriosis [7,17]. For this reason it is not possible to rule out uterine pathologies as a contributing cause of gene expression differences in the current study. However, there were subjects from both the PeriM and PreM groups that had uterine pathologies present, which may have mitigated the effect of these pathologies on gene expression differences between age groups.

## Conclusions

In this study, we have identified eMSC in women undergoing the transition to menopause and have evaluated gene expression of eMSC and eSF from PeriM women compared to PreM women. Our major finding that eSF from PeriM demonstrate a distinct gene profile from PreM eSF, while eMSC from PreM and PeriM women are quite similar, suggests that the changing hormonal milieu during the transition to menopause has a demonstrable effect on eSF gene expression and a minimal effect on the eMSC population. These data provide insight into these endometrial cell populations during the transition to menopause and offer a window into the mechanisms by which the endometrium maintains functional capacity even after menopause and potentially predisposing to abnormalities with compromised eSF functions in modulating E2 actions and other regulatory mechanisms.

We hypothesized that despite the changing hormonal milieu of the PeriM endometrium, eSF maintain functional capacity similar to PreM eSF. Our findings indicate, however, that PeriM eSF resemble more eMSC in gene signature than they do PreM eSF. This would suggest that the ability of the PeriM eSF to function in a similar manner to PreM eSF is impaired and additional studies to determine how PeriM eSF respond to sex hormones need to be performed. Analysis of the subject information in Table 1 reveals that PeriM subjects are on average older (47.9 yrs vs. 32.4 yrs, $P < 0.001$) and have lower average AMH levels (0.22 vs. 4.08 ng/ml, $P < 0.01$), with no significant differences in body mass index or circulating E2 and P4 levels. As circulating AMH levels tend to be lower in menopausal women, we can presume that these women are truly PeriM given that several have reported irregular menstrual cycles. However, we do not know the regularity of the cycles and only have a snapshot of hormonal data at a single point during the menstrual cycle in these women; we do not know for sure if the differences in gene expression observed in PeriM vs. PreM eSF are due to a differential stimulation of the cells by sex hormones in PeriM women or if these are the cumulative effects of hormone variation during irregular menstrual cycles. This needs to be addressed experimentally in the future. The apparent reduced differentiation of the PeriM eSF may also predispose the cells to variable response to hormone stimulation compared to PreM eSF, potentially leading to endometrial abnormalities in menopause. This idea also needs to be investigated further, using direct hormone stimulation of eSF from PeriM women in order to better understand the function of the PeriM eSF.

## Supplementary data

Supplementary data are available at *BIOLRE* online.

**Supplemental Table S1.** Differentially expressed genes in PeriM eMSC vs. PeriM eSF.
**Supplemental Table S2.** Differentially expressed genes in PeriM eMSC vs. PreM eMSC.
**Supplemental Table S3.** Differentially expressed genes in PeriM eSF vs. PreM eSF.
**Supplemental Table S4.** Differentially expressed genes in PreM eSF vs. PreM eMSC.

**Supplemental Table S5.** Predicted regulation (activated [Z-score ≥ 2.0] and suppressed [Z-score ≤ –2.0]) biological pathways by Ingenuity pathway analysis in PreM eSF vs. PreM eMSC.
**Supplemental Table S6.** Predicted regulation (activated [Z-score ≥ 2.0] and suppressed [Z-score ≤ –2.0]) biological pathways by Ingenuity pathway analysis in PeriM eMSC vs. PreM eMSC.
**Supplemental Table S7.** Predicted regulation (activated [Z-score ≥ 2.0] and suppressed [Z-score ≤ –2.0]) biological pathways by Ingenuity pathway analysis in PeriM eSF vs. PeriM eMSC.
**Supplemental Table S8.** Predicted regulation (activated [Z-score ≥ 2.0] and suppressed [Z-score ≤ –2.0]) biological pathways by Ingenuity pathway analysis in PeriM eSF vs. PreM eSF.

## Acknowledgments

The authors would like to acknowledge Kim Chi Vo of the UCSF NIH Human Endometrial Tissue and DNA Bank for assistance with tissue collection and processing, and Linda Ta and Yanxia Hao of the Genomics Core at the Gladstone Institute for assistance with microarray sample processing.

## References

1. Gargett CE, Masuda H. Adult stem cells in the endometrium. *Mol Hum Reprod* 2010; **16**:818–834.
2. Du H, Taylor HS. Contribution of bone marrow-derived stem cells to endometrium and endometriosis. *Stem Cells* 2007; **25**:2082–2086.
3. Cervello I, Gil-Sanchis C, Mas A, Simon C. Current understanding of endometrial stem cells. *Expert Rev Obstet Gynecol* 2009; **4**:273–282.
4. Spitzer TLB, Rojas A, Zelenko Z, Aghajanova L, Erikson DW, Barragan F, Meyer M, Tamaresis JS, Hamilton AE, Irwin JC, Giudice LC. Perivascular human endometrial mesenchymal stem cells express pathways relevant to self-renewal, lineage specification, and functional phenotype. *Biol Reprod* 2012; **86**:58, 1–16.
5. Gargett CE, Schwab KE, Zillwood RM, Nguyen HPT, Wu D. Isolation and culture of epithelial progenitors and mesenchymal stem cells from human endometrium. *Biol Reprod* 2009; **80**:1136–1145.
6. Schwab KE, Gargett CE. Co-expression of two perivascular cell markers isolates mesenchymal stem-like cells from human endometrium. *Hum Reprod* 2007; **22**:2903–2911.
7. Barragan F, Irwin JC, Balayan S, Erikson DW, Chen JC, Houshdaran S, Piltonen TT, Spitzer TLB, George A, Rabban JT, Nezhat C, Giudice LC. Human endometrial fibroblasts derived from mesenchymal progenitors inherit progesterone resistance and acquire an inflammatory phenotype in the endometrial niche in endometriosis. *Biol Reprod* 2016; **94**:118, 1–20.
8. Sitruk-Ware R. New hormonal therapies and regimens in the postmenopause: routes of administration and timing of initiation. *Climacteric* 2007; **10**:358–370.
9. NAMS Recommendations for Clinical Care of Midlife Women Working GroupShifren JL, Gass, ML. The North American Menopause Society recommendations for clinical care of midlife women. *Menopause* 2014; **21**:1038–1062.
10. Luukkainen T. The levonorgestrel intrauterine system: therapeutic aspects. *Steroids* 2000; **65**:699–702.
11. Sitruk-Ware R, Inki P. The levonorgestrel intrauterine system: long-term contraception and therapeutic effects. *Womens Health* 2005; **1**:171–182.
12. Long ME, Faubion SS, MacLaughlin KL, Pruthi S, Casey PM. Contraception and hormonal management in the perimenopause. *J Womens Health* 2015; **24**:3–10.
13. Hale G, Paul-Labrador M, Dwyer JH, Merz CNB. Isoflavone supplementation and endothelial function in menopausal women. *Clin Endocrinol (Oxf)* 2002; **56**:693–701.
14. Ubaldi F, Rienzi L, Baroni E, Ferrero S, Iacobelli M, Minasi MG, Sapienza F, Martinez F, Cobellis L, Greco E. Implantation in patients over 40 and raising FSH levels–a review. *Placenta* 2003; **24**:S34–S38.
15. Navot D, Drews MR, Bergh PA, Guzman I, Karstaedt A, Scott RT, Garrisi GJ, Hofmann GE. Age-related decline in female fertility is not due to diminished capacity of the uterus to sustain embryo implantation. *Fertil Steril* 1994; **61**:97–101.
16. Ulrich D, Tan KS, Deane J, Schwab K, Cheong A, Rosamilia A, Gargett CE. Mesenchymal stem/stromal cells in post-menopausal endometrium. *Hum Reprod* 2014; **29**:1895–1905.
17. Piltonen TT, Chen J, Erikson DW, Spitzer TLB, Barragan F, Rabban JT, Huddleston H, Irwin JC, Giudice LC. Mesenchymal stem/progenitors and other endometrial cell types from women with polycystic ovary syndrome (PCOS) display inflammatory and oncogenic potential. *J Clin Endocrinol Metab* 2013; **98**:3765–3775.
18. Mazan-Mamczarz K, Hagner PR, Dai B, Wood WH, Zhang Y, Becker KG, Liu Z, Gartenhaus RB. Identification of transformation-related pathways in a breast epithelial cell model using a ribonomics approach. *Cancer Res* 2008; **68**:7730–7735.
19. Smith-McCune K, Chen JC, Greenblatt RM, Shanmugasundaram U, Shacklett BL, Hilton JF, Johnson B, Irwin JC, Giudice LC. Unexpected inflammatory effects of intravaginal gels (Universal Placebo Gel and Nonoxynol-9) on the upper female reproductive tract: a randomized crossover study. *PloS One* 2015; **10**:e0129769.
20. Peart MJ, Smyth GK, van Laar RK, Bowtell DD, Richon VM, Marks PA, Holloway AJ, Johnstone RW. Identification and functional significance of genes regulated by structurally different histone deacetylase inhibitors. *Proc Natl Acad Sci U S A* 2005; **102**:3697–3702.
21. Raouf A, Zhao Y, To K, Stingl J, Delaney A, Barbara M, Iscove N, Jones S, McKinney S, Emerman J, Aparicio S, Marra M et al. Transcriptome analysis of the normal human mammary cell commitment and differentiation process. *Cell Stem Cell* 2008; **3**:109–118.
22. Huggins CE, Domenighetti AA, Ritchie ME, Khalil N, Favaloro JM, Proietto J, Smyth GK, Pepe S, Delbridge LMD. Functional and metabolic remodelling in GLUT4-deficient hearts confers hyper-responsiveness to substrate intervention. *J Mol Cell Cardiol* 2008; **44**:270–280.
23. Dalman MR, Deeter A, Nimishakavi G, Duan ZH. Fold change and *P*-value cutoffs significantly alter microarray interpretations. *BMC Bioinformatics* 2012; **13**:S11.
24. Cunha GR, Bigsby RM, Cooke PS, Sugimura Y. Stromal-epithelial interactions in adult organs. *Cell Differ* 1985; **17**:137–148.
25. Snijders MP, de Goeij AF, Debets-Te Baerts MJ, Rousch MJ, Koudstaal J, Bosman FT. Immunocytochemical analysis of oestrogen receptors and progesterone receptors in the human uterus throughout the menstrual cycle and after the menopause. *J Reprod Fertil* 1992; **94**: 363–371.
26. Lessey BA, Killam AP, Metzger DA, Haney AF, Greene GL, McCarty KS. Immunohistochemical analysis of human uterine estrogen and progesterone receptors throughout the menstrual cycle. *J Clin Endocrinol Metab* 1988; **67**:334–340.
27. Gargett CE, Chan RW, Schwab KE. Hormone and growth factor signaling in endometrial renewal: role of stem/progenitor cells. *Mol Cell Endocrinol* 2008; **288**:22–29.
28. Koehler KF, Helguero LA, Haldosén LA, Warner M, Gustafsson JA. Reflections on the discovery and significance of estrogen receptor beta. *Endocr Rev* 2005; **26**:465–478.
29. Critchley HO, Brenner RM, Henderson TA, Williams K, Nayak NR, Slayden OD, Millar MR, Saunders PT. Estrogen receptor beta, but not estrogen receptor alpha, is present in the vascular endothelium of the human and nonhuman primate endometrium. *J Clin Endocrinol Metab* 2001; **86**:1370–1378.
30. Matsuzaki S, Uehara S, Murakami T, Fujiwara J, Funato T, Okamura K. Quantitative analysis of estrogen receptor alpha and beta messenger ribonucleic acid levels in normal endometrium and ovarian endometriotic cysts using a real-time reverse transcription-polymerase chain reaction assay. *Fertil Steril* 2000; **74**:753–759.
31. Pedeutour F, Quade BJ, Weremowicz S, Dal Cin P, Ali S, Morton CC. Localization and expression of the human estrogen receptor beta gene in uterine leiomyomata. *Genes Chromosomes Cancer* 1998; **23**:361–366.

32. Mathieu PS, Loboa EG. Cytoskeletal and focal adhesion influences on mesenchymal stem cell shape, mechanical properties, and differentiation down osteogenic, adipogenic, and chondrogenic pathways. *Tissue Eng Part B Rev* 2012; **18**:436–444.
33. Rodier F, Campisi J. Four faces of cellular senescence. *J Cell Biol* 2011; **192**:547–556.
34. Mannoor K, Liao J, Jiang F. Small nucleolar RNAs in cancer. *Biochim Biophys Acta* 2012; **1826**:121–128.
35. Vogelstein B, Lane D, Levine AJ. Surfing the p53 network. *Nature* 2000; **408**:307–310.
36. Vousden KH. Activation of the p53 tumor suppressor protein. *Biochim Biophys Acta* 2002; **1602**:47–59.
37. Peffers MJ, Liu X, Clegg PD. Transcriptomic profiling of cartilage ageing. *Genomics Data* 2014; **2**:27–28.
38. Heberle H, Meirelles GV, da Silva FR, Telles GP, Minghim R. InteractiVenn: a web-based tool for the analysis of sets through Venn diagrams. *BMC Bioinformatics* 2015; **16**:169.